Ab Initio Comparative Study of the Structure and Properties of H_2-Porphin and H_2-Phthalocyanine. The Electronic Absorption Spectra

H. Cortina

Centro de Investigaciones de Energía Solar, c) Micro 3, Reparto Abel Santamaría,
Santiago de Cuba, 90800 Cuba

M. L. Senent* and Y. G. Smeyers

Departamento de Quimica y Física Teóricas, I. Estructura de la Materia, CSIC,
Serrano 113b, Madrid 28006, Spain

Received: March 21, 2003; In Final Form: July 17, 2003

The structure and properties of free base porphin (PH_2) and phthalocyanine (PcH_2) are compared using B3LYP/6-31G(d,p) (5D) and UHF/6-31G(d,p) (5D) calculations. The two molecules show two isomers where the two central hydrogen atoms lie in trans and cis positions. The C_{2v} cis-isomers lie 2840 cm^{-1} (PH_2) and 3183 cm^{-1} (PcH_2) over the most stable D_{2h} trans-geometries. The tautomerization processes are hindered by transition states at 5269 cm^{-1} (PH_2) and 5107 cm^{-1} (PcH_2). The ionization potential and the electron affinity are calculated to be +6.40 and −1.11 eV for PH_2 and +6.03 and −1.91 eV for PcH_2, from the determination of the cation and anion energies and structures. Harmonic frequencies and electric and nonlinear optical properties are also reported. An interpretation of the electronic absorption spectra is also given for both molecules. For PH_2, CASPT2 calculations have been achieved using the 6-31G(d,p) (5D) base set and different active spaces. For PcH_2, the spectrum has been interpreted at the CASPT2(4,4)/6-31 level. The calculated positions of the Q_x, Q_y, and B bands of phthalocyanine (1.61, 1.99, and 3.14 and 3.19 eV) are in a very good agreement with the experimental values (1.81, 1.99, and 3.65 eV).

Introduction

Porphyrins and phthalocyanines play important roles in many biological mechanisms for their physical and chemical properties.[1,2] As photosynthesis is one of the most significant examples of this characteristic process, their study is of interest for the development of new organic materials for optoelectronic and artificial solar energy conversion.[3]

The variety and significance of properties and applications arise from the characteristic molecular structures. Free base porphin (PH_2) and free base phthalocyanine (PcH_2) (see Figures 1a and 2a) can be contemplated as the fundamental components of the two series of compounds. From the theoretical point of view, the high symmetry and π-delocalitation have induced their investigation. Structures, properties, and applications can be modified and modulated by introducing metals in the macrocyclic cavity or adding axial and peripherical substituted.[2,3]

An exhaustive understanding of the free base compounds is fundamental for the search of new organic materials composed by porphyrins and phthalocyanines. For this reason, the main purpose of this paper is to compare PH_2 and PcH_2 and to obtain as much relevant information as possible from quantum-mechanical calculations. For this purpose, stable structures and optical and spectroscopic properties are determined, and the absorption spectra, related to the electronic transfer processes, are also analized. Although some attended aspects of PH_2 have been first studied with more or less sophisticated calculations,[4−25] the present theoretical investigation of the structure and spectrum of PcH_2 is innovative. To our knowledge, few calculations performed using effective Hamiltonians have been published.[26−28] The main available spectroscopic and structural information of PcH_2 is experimental.[29−34]

PH_2 presents two stable structures trans and cis (see Figure 1a,b).[12,25] The determination of the trans-conformer symmetry has been the object of many theoretical investigations over a long period. Previous papers show a long discussion concerning the relative stability of two possible trans-minima: a C_{2v} geometry, which represents a resonant structure where single and double bonds are alternated, and a D_{2h} geometry, where all the bonds are balanced.[5−7,9,10] The complexity of the study proceeds from the high-symmetry structure, the π-delocalitation, and the relative large size of PH_2, which induce instabilities in the ab initio calculations. The near-degeneration of the orbitals produces RHF unstable functions and false relative energy. At this level, PH_2 presents two C_{2v} favorite geometries separated by a saddle point of D_{2h} symmetry. X-ray[35] and NMR[36] measures of substituted porphyrins prove that *trans*-PH_2 is a highly symmetric molecule.

Similar behavior can be expected for PcH_2, which shows a high density of states close to the ground state. This molecule has been studied by neutron and X-ray diffraction.[29−31] The neutron diffraction structural data have been interpreted by assuming a D_{2h} symmetry,[30] where the two hydrogens are localized on opposite nitrogen atoms. The earlier X-ray study of the solid state was interpreted with a hydrogen-bridge model where the hydrogens are shared by two nitrogen atoms.[29,31]

The instability of the RHF functions in conjugated systems is a well-known effect[35] that was first studied in PH_2 by Reynolds using semiempirical methods.[5] Previous papers on

---

* Corresponding author. E-mail: imts420@iem.cfmac.csic.es.

10.1021/jp0347320 CCC: $25.00

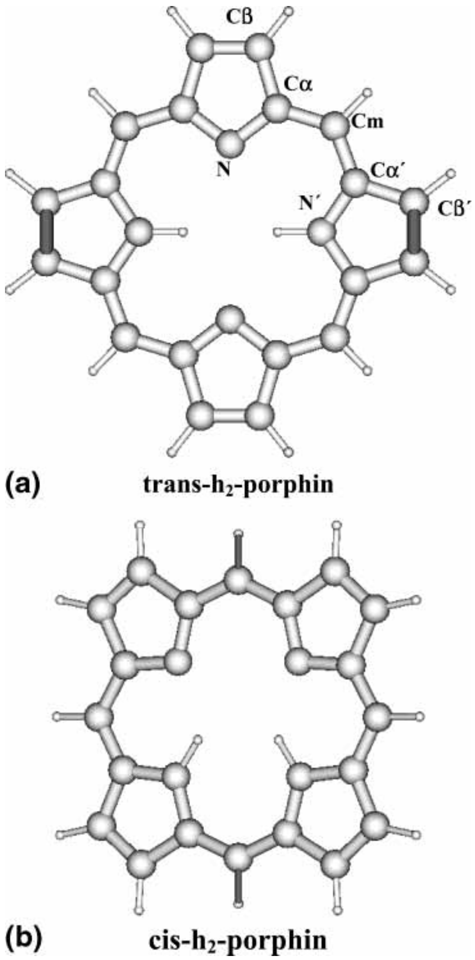

Figure 1. *trans*-H_2-Porphin (a) and *cis*-H_2-porphin (b).

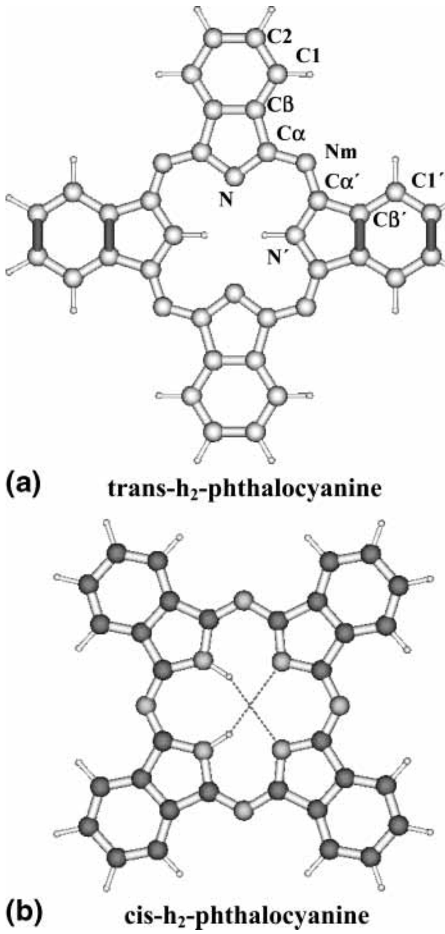

Figure 2. *trans*-H_2-Phthalocyanine (a) and *cis*-H_2-phthalocyanine (b).

trans-PH_2[5−7,9,10] recognized an important job for the electron correlation. Almöf et al.,[8] authors of one of the most complete works, have compared the RHF, MP2/RHF, and LDF behaviors starting the search from C_{2v} and D_{2h} geometries. From the negative eigenvalues of the stability matrix, they found an UHF determinant lying below the RHF one. They have obtained a unique D_{2h} minimum with MP2 and LDF but have ignored the fact that the reference determinant instability can be retained by the correlated functions. Merchan et al.,[10] following the four orbital model of Gouterman,[30−32] have performed CASPT2 calculations on two C_{2v} and D_{2h} structures of porphin. The D_{2h} geometry is found to be the most stable when the π and σ electrons are simultaneously correlated. The multireference description is comparable to the derived from Möller−Plessset theory applied on a single Slater determinant.

The spectroscopic properties of PH_2 and PcH_2 have very much interest from the theoretical point of view, and for their applications in optoelectronic and solar energetic. The electronic absorption spectrum of PH_2[39−45] shows three different regions with $\pi-\pi^*$ transitions. The first one corresponds to the visible and shows a Q pattern with two components: Q_x (parallel polarization and very weak) is observed between 1.98 and 2.02 eV, and Q_y (perpendicular polarization and high intensity) is observed between 2.33 and 2.43 eV. The second region, at the near-ultraviolet, shows a very intense B band called Soret between 3.13 and 3.33 eV. The third region shows broad and diffuse bands (N (at 3.65 eV) and L (at 4.25 eV)).

The four orbital model of Gouterman[38−40] has been the conventional model for the absorption spectrum interpretation because the main effect of the π-orbitals near-degeneration appears in the last occupied and the first unoccupied orbitals. The two high occupied orbitals (HOMO and HOMO−1) transform as the b_{1u} and au representations of the D_{2h} group, whereas the two lowest virtual orbitals (LUMO and LUMO+1) show b_{2g} and b_{3g} symmetries. The excitations connecting these orbitals produce two B_{2u} and two B_{3u} electronic states and provide two parallel bands Q_x and B_x and two perpendicular bands Q_y and B_y. According to this interpretation, the Soret B band is assumed to be composed of two perpendicular components.

Many authors, who have employed ab initio calculations for the assignments, have taken into consideration the Gouterman model. Nagashima et al.[4] and Yamamoto et al.[8] have used interaction configuration (CISD), whereas Merchan et al.[11−19] have employed second-order perturbation theory on different active spaces (CASPT2). They concluded that the simultaneous correlation of π and σ electrons is crucial for reproducing experimental band positions and geometries. The CASPT2 results are almost independent of the CAS size.

The B band assignment has induced controversy because experiments show a unique branch, and calculations based on the four orbital model distinguish two B_x and B_y components.[4,8,11,19] Serrano-Andrés et al.[19] have related the discrepancies to the basis set. They have demonstrated that the enlargement approaches the second B_{3u} to the second B_{2u} excited state. Recently, a new assignment has been proposed: Nakatsuji et al.[16] and Nooijen and Barlett[17] have related the excitation $1A_g-2B_{3u}$ to the B band and the transition $1A_g-2B_{2u}$ to the N band. They use SAC-CI and STEOM-CC methods. Later, Gwaltney and Barltlett[20] have returned to the old interpretation although their STEOM-CC results are in a very good agreement with those of ref 17. The spectrum has been also interpreted using density functional theory.[22,24]

In the case of PcH_2, the large size of the molecule has hindered the rigorous interpretation of the spectrum.[32,33] It shows two sharp peaks in the visible region at 686 nm (1.81 eV) (Q_x) and 622 nm (1.99 eV) (Q_y) (Q-band), a less intense broad band centered at 340 nm (3.65 eV) and extended from 376 to 302 nm (Soret or B band), and other bands (N, L, and C) below 280 nm. Theoretical studies with valence effective Hamiltonians show two intense optical transitions in the visible region that can be clearly correlated with the components Q_x and Q_y.

Although, the four orbital model proposed for PH_2 has been considered inadequate to interpret the B band of PcH_2,[27,28] the current work is a study of the spectrum and the validity of the model using CASPT2 calculations over a CAS(4,4) active space. The spectrum is calculated and compared with the one of free base porphin. The vibrational spectrum is also analyzed. We report structures and properties of PcH_2 and, for the first time, the harmonic frequencies. The vibrational spectrum of PH_2 is also calculated and interpreted from ab initio methods.[6,13−15,23]

Structure and Molecular Properties of H_2-Porphin and H_2-Phthalocyanine

For comparing the two molecules, the calculations have been achieved at the same level of theory imposed by the size of PcH_2. The computations of structures and properties have been performed with the Gaussian 98 program.[46]

The search of minimum energy structures of trans-free base porphin and trans-free base phthalocyanine has been initialized with the RHF/6-31G(d,p) (5D) method and full optimization of the geometry. The 6-31G(d,p) (5D) basis set contains 406 atomic orbitals and 770 primitive functions in the case of PH_2, and 650 orbitals and 1246 Gaussian functions for PcH_2. Geometry optimizations have been started from four C_s, C_{2v}, and D_{2h} geometries by imposing symmetry constrains. As was expected, the four initial geometries converge to two planar structures of C_{2v} and D_{2h} symmetry. The C_{2v} symmetry has been found to be the most stable in disagreement with the experimental measures.

The first column of Table 1 shows the RHF/6-31G(d,p) (5D) energies of the neutral molecules and the ionic species. The cation and anion structures and energies have been integrated for obtaining electron affinities and ionization potentials with orbital and geometry relaxation. The PH_2 total electronic energies have been determined to be −983.285366 au (C_{2v}) and −983.279313 (D_{2h}) au, and the ones of PcH_2, to be −1657.936390 au (C_{2v}) and −1657.929076 au (D_{2h}). The energy differences between the two symmetries, 1328.5 cm^{-1} for PH_2 and 1605.0 cm^{-1} for PcH_2, are of an order of magnitude corresponding to different conformations. Apparently, they are critical points of the potential energy surface of the electronic ground state. However, the gaps of the third column (energy differences between the lowest virtual and the highest occupied orbitals) show clearly that the two C_{2v} and D_{2h} forms correspond to different electronic configurations. For PH_2, Δgap is 0.8 eV (0.26758−0.23637 au). For PcH_2, Δgap is 0.8 eV (0.21562−0.18440 au).

For both molecules, the RHF harmonic analysis proves that the C_{2v} geometry represents a potential energy surface minimum, whereas the D_{2h} structure is a transition state. Ignoring the orbital energies, it looks like a saddle point between two Kekule C_{2v} structures. For both molecules, the D_{2h} geometries show one negative frequency that transforms as the B_{3u} representation and corresponds to A_1 skeletal deformation in the C_{2v} structures.

TABLE 1: Total Electronic Energies *E* (au), Relative Energies E_R (cm^{-1}), HOMO−LUMO Gap (au) of *trans*-PH_2 and *trans*-PcH_2 Calculated with HF, UHF+stable and the 6-31G (5D) Basis Set**

	HF			UHF+opt
	E	E_R	gap	*E*
		PH_2		
C_{2v}	−983.285366	0.0	0.26758	
D_{2h}	−983.279313	1328.5	0.23637	−983.339229
		PH_2^{1-}		
C_{2v}	−983.313289	0.0	0.25379	−983.325652
D_{2h}	−983.294740	4071.0	0.22140	
		PH_2^{1+}		
C_{2v}	−983.116444	0.0	0.23110	
D_{2h}	−983.103411	2860.4	0.16075	−983.122583[a]
		PcH_2		
C_{2v}	−1657.936390	0.0	0.21562	−1658.008226
D_{2h}	−1657.929076	1605.0	0.18440	−1658.008787[a]
		PcH_2^{1-}		
C_{2v}	−1658.002590	0.0	0.24408	
D_{2h}	−1657.977891	5420.8	0.16109	.1658.024849[a]
		PcH_2^{1+}		
C_{2v}	−1657.265258	22530.4	0.07021	
D_{2h}	−1657.779811	0.0	0.20412	−1657.812517[a]

[a] Asymmetric structures.

Inconsistencies and divergencies with experimental results[35,36] came from the RHF function instability caused by the small gap between orbitals, the π-delocalitation and the high symmetry of the molecules. For exploring the problem, we have restarted the investigation following two different ways and using the RHF symmetrical geometries to reinitialize the calculations. For determining and comparing molecular properties, we use density functional theory (B3LYP/6-31G(d,p) (5D)), which produces stable functions; for exploring the instabilities, we use the algorithms implemented in Gaussian98,[47] which produces UHF functions after taking away the constrains of the RHF method. As was first inquired by Reynolds[5] and Almlöf et al.[9] for the neutral *trans*-PH_2, a UHF determinant more stable than the RHF one exists for both molecules. In the case if the ionic species, an UHF determinant of low symmetry exists below the symmetrical one. Although they are inconsistent, the RHF and UHF results are included in the tables because they can be useful for understanding of the π-electronic structure of porphyrins.

In the fourth column of Table 1, the energies obtained after eliminating constrains of the RHF method (UHF+opt) are shown.[47] They correspond to the minimum energy structures, all the frequencies of which are positive. They have been calculated by optimizing the geometries starting from the RHF minima and using the corresponding optimized UHF determinants as initial guesses. In the process, some structures lose the original symmetry. If the symmetry break appears only on the high virtual orbitals, the molecules maintain D_{2h} properties. This is the case of the UHF+opt unique minimum of PH_2 (E = −983.339229 au) that shows a dipole moment equal to zero. Although the UHF+opt method is not optimum, it may be regarded as a valid approximation for calculating properties connected with the electronic structure. For example, in PH_2, the ionization potential improves significantly with the wave function optimization (from 4.8 eV (RHF) to 5.9 eV (UHF+opt). The experimental value is 6.9 eV[48]).

From the contributions of the nuclear repulsion energy (N−N), the one-electron energy (E), and the electron kinetic energy (KE) to the total RHF and UHF+opt energies, it may be inferred that an electron delocalization gain is the physical

TABLE 2: Total Electronic Energies (au), Relative Energies (cm^{-1}), HOMO−LUMO Gap (au) of *trans*- and *cis*-PH_2 and *trans*-PcH_2 Calculated with B3LYP/ 6-31G (5D)**

	PH_2			PcH_2		
	E_a	E_R	gap	E_a	E_R	gap
trans (D_{2h})	−989.556491	0	0.10702	−1668.329426	0	0.07889
cis (C_{2v})	−989.543551	2840	0.10610	−1668.314923	3183	0.08007
TS (C_s)	−989.532483	5269	0.10659	−1668.306158	5107	0.07823
trans-PH_2^{1-}	−989.592561		0.04056	−1668.395845		0.04188
trans-PH_2^{1+}	−989.319129		0.04876	−1668.107603		0.07907

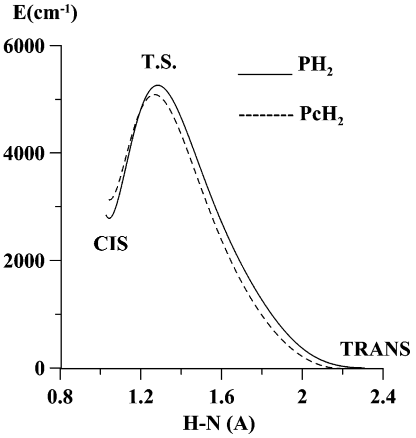

Figure 3. Minimum energy path of the tautomerization process.

TABLE 3: Structural Parameters[a] of PH_2 and PcH_2

		trans-PH_2			
H−N′	1.0148	H−N′−C_α′	124.6	TS	
N′−C_α′	1.3724	N′−C_α′−C_β′	106.6	H−N1	1.0258
N−C_α	1.3635	N−C_α−C_β	111.1	H−N2	1.2841
C_α′−C_β′	1.4350	Cm−C_α′−C_β′	127.9	H−N3	1.2682
C_α−C_β	1.4606	Cm−C_α−C_β	123.3	N2−H−N1	147.2
C_α′−Cm	1.3940	C_α′−Cm−C_α	127.1		
C_α−Cm	1.4002	C_β′−C_β′−C_α′	108.0	*cis*-PH_2	
C_β′−C_β′	1.3724	C_β′−C_β′−C_α′	106.2	H−N	1.0283
C_β−C_β	1.3564	H−C_β′−C_α′	124.3	H−N−C_α	117.0
H−C_β′	1.0815	H−C_β−C_α	125.4		
H−C_β	1.0827	H−Cm−C_α′	115.9		
H−Cm	1.0860				
		trans-PcH_2			
H−N′	1.0135	H−N′−C_α′	123.8	TS	
N′−C_α′	1.3780	N′−C_α′−C_β′	106.2	H−N1	1.0265
N−C_α	1.3654	N−C_α−C_β	121.4	H−N2	1.2660
C_α′−C_β′	1.4528	C_α′−C_β′−C_1′	131.4	H−N3	1.3347
C_α−C_β	1.4670	C_α−C_β−C_1	133.1	N2−H−N1	143.8
C_α′−Nm	1.3180	C_β′−C_1′−C_2′	117.8		
C_α−Nm	1.3363	C_β−C_1−C_2	117.6	*cis*-PcH_2	
C_1′−C_β′	1.3978	C_2−C_2′−C_β′	121.2	H−N	1.0305
C_1−C_β	1.3929	C_2−C_2−C_β	121.1	H−N−C_α	115.3
C_1′−C_2′	1.3915	Nm−C_α′−C_α′	125.7		
C_1−C_2	1.3972	Nm−C_α−C_β	121.4		
C_2′−C_2′	1.4106	C_α−Nm−C_α′	123.8		
C_2−C_2	1.4057	C_β′−C_1′−H	120.4		
H−C_1′	1.0849	C_β−C_1−H	120.8		
H−C_1	1.0852	H−C_2′−C_1′	119.6		
H−C_2′	1.0860	H−C_2−C_1	119.6		
H−C_2′	1.0863				

[a] Distances in Å; angles in degrees.

meaning of the elimination of the RHF constrains ($N-N_{RHF} = 1868.4339$ au, $E_{RHF} = -5048.7773$ au, $KE_{RHF} = 983.1177$ au and $N-_{UHF+opt} = 1853.9115$ au, $E_{UHF+opt} = -5020.1907$ au, $KE_{UHF+opt} = 983.2278$ au). The effect is larger for PH_2 ($\Delta N-N = 0.78\%$, $\Delta E = 0.57\%$, $\Delta KE = 0.01\%$) than for PcH_2 ($\Delta N-N = 0.61\%$, $\Delta E = 0.47\%$, $\Delta KE = 0.01\%$). ($\Delta N-N = |N-N_{RHF} - N-N_{UHF+opt}| \times 100/N-N_{RHF}$, ...).

Table 2 shows the critical point energies of the two molecules calculated with B3LYP/6-31G(d,p) (5D). At this level of theory, which produces stable functions, the most stable structures are trans-isomers of D_{2h} symmetry. Both molecules shows a secondary minimum of C_{2v} symmetry where the two central hydrogens are attached to neighboring nitrogens (see Figure 2a,b). The separation of the two isomers has been calculated to be 2840.1 cm^{-1}, for PH_2, and to be 3183.0 cm^{-1}, for PcH_2.

In the first papers, the X-ray data of PcH_2[29−31] were interpreted using a hydrogen-bridge model where each hydrogen is shared by two neighboring atoms. Our calculations show that this structure represents a step of maximum energy of the trans: cis transformation process. Nevertheless, the interpretation of Hoskins et al.[30] is supported by the DFT calculations.

In the trans-isomer, the two central hydrogens can lie in the axis z or y. In the cis-isomers, the two hydrogens can be connected to neighboring nitrogens in four different ways. Although the tautomerism mechanism between the two trans-forms of PH_2 has been the object of controversy, calculations, and experiments denote that it is a two-step process.[12−25] The stability of the cis-isomers, which shows all the frequencies positive, suggests a mechanism as *trans*-PH_2 (z):*cis*-PH_2:*trans*-PH_2 (y) for both molecules.

Figure 3 represents the minimum energy path of the tautomerization processes. The independent variable N−H represents a real bond of the cis-isomer breaking during the process. The path has been calculated from the energies of 10 structures partially optimized. The N−H distance has been frozen whereas the orientation has been relaxed. The relative energy of the transition states with respect to the trans-forms have been calculated to be 5269 cm^{-1} for PH_2 and 5107 cm^{-1} for PcH_2, and the N−H distances to be 1.2841 Å in PH_2 and 1.2660 Å in PcH_2. From the thermodynamic point of view, the cis-isomer formation is slightly more probable for PH_2 than for PcH_2, whereas, from the kinetic point of view, the activation energy favors the PcH_2 process. It may be inferred that both molecules present similar behavior.

Table 3 shows the structural parameters of *trans*-PH_2 and *trans*-PcH_2 and the same characteristic bond distances and angles of the cis-form and the transition state. Tables 4 and 5 show the molecular properties and the harmonic frequencies. If we compare the rotational constants of the trans and cis-isomers, it is evident that PH_2 is more distorted during the tautomerization than PcH_2.

The ionization potentials (IP) and the electron affinities (E_a) are magnitudes of interest to evaluate the possibility of applications of molecular systems in the profit of solar energy. To include geometry and orbital relaxation, they have been determined from the zero point energies (ZPE) of the neutral species, cations, and anions (see Table 4). For this purpose, the cation and anion geometries have been fully optimized using as starting points the neutral trans-species structures. For both molecules, two processes *trans*-PH_2:*trans*-PH_2^{1+} and *trans*-PH_2:*trans*-PH_2^{1-} have been considered.

If the relaxation is allowed, the B3LYP/6-31G(d,p) (5D) ionization potentials are 6.40 eV (PH_2) and 6.03 eV (PcH_2) and

TABLE 4: Zero-Point Energy (ZPE, au), Ionization Potential (IP, eV), Electron Affinity (E_a, eV), Dipole Moment (Debye), Polarizabilities (au), and Hyperpolarizabilities (au) of PH_2 and PcH_2 Calculated with B3LYP/6-31G (5D)**

	trans-PH_2 (D_{2h})	*cis*-PH_2 (C_{2v})	*trans*-PcH_2 (D_{2h})	*cis*-PcH_2 (C_{2v})
ZPE	−989.260301	−989.248070	−1667.892769	−1667.879229
A (MHz)	266.1308	278.9281	89.2738	89.3686
B (MHz)	263.5992	251.3367	88.9665	88.8999
C (MHz)	132.4295	132.2073	44.5599	44.5668
IP[a,b]	6.40		6.03	
E_a[b]	−1.11		−1.91	
μ	0.0000	2.0932	0.0000	1.9367
α_{xx}	446.7	428.2	846.3	828.6
α_{yy}	434.9	455.3	829.0	828.4
α_{zz}	73.1	73.2	114.9	114.9
β_{zzz}	0.000	0.000	0.000	0.000
β_{zzy}	−0.079	0.000	−0.544	−0.000
β_{zyy}	0.079	0.000	0.544	0.000
β_{yyy}	−0.237	0.000	−1.632	0.000
β_{zzx}	−4.351	9.054	7.548	2.946
β_{zyx}	1.927	−3.907	−5.580	−6.5426
β_{yyx}	−3.155	−134.248	0.748	493.969
β_{zxx}	4.351	−8.6706	−7.548	−6.546
β_{yxx}	3.155	1.5448	−0.748	2.975
β_{xxx}	−0.897	16.744	−2.509	−3536.663

[a] Experimental IP: IP = 6.9 eV[40] (for PH_2); IP = 6.41 eV[41] (for PcH_2). [b] ZPE of the anions = −989.301062 au (PH_2^{-1}), −1167.962876 au (PcH_2^{-1}); ZPE of the cations = −989.025268 au (PH_2^{-1}), −1167.671359 au (PcH_2^{-1}).

the electron affinities are −1.11 eV (PH_2) and −1.91 eV (PcH_2). In agreement with experiments, IP is 0.37 eV larger in PH_2 than in PcH_2. The observed values are 6.9 eV (PH_2)[40] and 6.41 eV (PcH_2),[41] which represent a difference of 0.49 eV. The IP is underestimated with DFT, whereas a considerable improvement is obtained if orbitals and geometry are relaxed. With the Koopman's theorem ($IP = -E_{HOMO(B3LYP)}$), we obtain 5.16 eV (PH_2) and 4.98 eV (PcH_2). Previous papers show that different ab initio techniques usually underestimate the IP value (for example, SAC-CI (6.09 eV,[16]), STEOM-PT (6.40 eV[17]). However, previous semiempirical calculations that include electron correlation overestimate the ionization potentials (7.30 eV (PH_2)[42]). With semiempirical correlated calculations, it has been found to be 6.57 eV).[42]

Applications of porphyrins and phthalocyanines in optoelectronic depend on their linear and nonlinear optical properties. The changes in optical and electrical properties of PH_2 and PcH_2 during interactions with other molecules have been the basis of chemical sensors transducer layers. As was expected, the D_{2h} structures' dipole moments are zero (Table 4) and the C_{2v} dipole moment of PcH_2 (1.9367 D) is larger than the one of PH_2 (2.0932 D), which is more distorted during the tautomerization. However, the components of the polarizability tensor and the hyperpolarizabilities are a 50% larger for PcH_2 because the gap between excited states of PcH_2 is smaller than in PH_2. The static hyperpolarizability components of Table 4 are calculated numerically. They cannot be directly compared with experiments but there are highly valuable to understand the influence of the molecular and electronic structures on hyperpolarizabilities.

Whereas the harmonic force field of the D_{2h} isomer of PH_2 has been first studied carefully,[6,13,15,23] to our knowledge, there are no published frequencies for PcH_2 (see Supporting Information). The harmonic frequencies can be calculated with UHF+opt if the symmetry of the lowest orbitals is preserved. For PH_2, the symmetry representations lowest modes have been calculated to be 156.7, 133,5, 125, 98.1, 66.8, 316.5, 292.1, 55.4 cm^{-1} with B3LYP and 159.5, 130.7, 115.7, 129.9, 72.9, 331.4, 322.2, 55.8 cm^{-1} with UHF+opt.

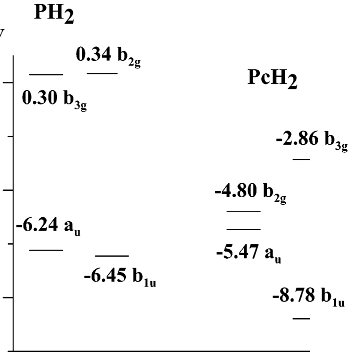

Figure 4. HOMO−1, HOMO, LUMO, and LUMO+1 orbitals of porphin and phthalocyanine.

Electronic Absorption Spectra of H_2-Porphin and H_2-Phthalocyanine

The absorption spectra have been investigated by determining the vertical excitations with the methods CAS (multiconfigurational using the completed active space) and CASPT2 (second-order multiconfigurational perturbation theory). The multiconfigurational computations have been performed with the code MOLCAS[51] on the B3LYP/6-31G(d,p) (5D) geometries.

The calculations of PH_2 were carried out with the 6-31G(d,p) (5D) basis set using different definitions of the active space. For the selection, we have started from the work of Serrano-Andrés et al.,[19] who have defined π-spaces with the lowest 6 virtual orbitals and 7 (or 8) occupied orbitals and conclude that the CASPT2 results do no depend on the size of the active space but on the nature of the included of excluded orbitals. For adding more information, we have selected new sets for incorporating all the π-occupied system. As orbitals over $4b_{3g}$ do not contribute to the transitions, we have limited the virtual space to 2 or 3 orbitals.

Table 5 shows the excitations energies obtained with different spaces. CAS(4,4) refers to Gouterman et al.'s model.[38−40] On the basis of the orbital gaps, four π-orbitals HOMO−1, HOMO, LUMO, and LUMO+1 have been selected. For CAS(5,4), the space has been augmented adding a virtual π-orbital of au symmetry (see Figure 4). In the cases of the CAS(8/12) and CAS(9/12) calculations, twelve electrons have been correlated and the space has been defined with six π-occupied orbitals and two or three virtual π-orbitals. In the CAS(15/26) case, all the occupied π-orbitals have been included. All the valence σ and π electrons have been correlated for the CASPT2 calculations.

The PH_2 spectrum is characterized by three patterns, corresponding to the regions between1.98 and 2.02 eV (Q_x band), 2.33 and 2.42 eV (Q_y band), and 3.13 and 3.33 eV (B band)

TABLE 5: Vertical Excitations Energies (eV) of PH_2

		CAS					CASPT2	CASPT2	
state	assign	(4/4)	(5/4)	(8/12)	(9/12)	(15/26)	(4/4)	(5/4)	exp
1 $^1B_{3u}$	Q_x	3.58	3.32	3.08	2.77	3.01	1.11	1.00	1.98−2.02
1 $^1B_{2u}$	Q_y	3.81	3.55	3.31	3.38	3.22	1.74	1.71	2.33−2.42
2 $^1B_{3u}$	B_x	5.20	5.12	4.60	4.55	4.56	3.87	2.22	3.13−3.33
2 $^1B_{2u}$	B_y	5.21	5.21	5.11	4.85	5.02	2.78	2.34	

TABLE 6: Comparison between Absorption Spectra of $PH_2$and PcH_2

		PH_2			PcH_2		
		CAS(4,4)	CASPT2(4,4)	exp	CAS(4,4)	CASPT2(4,4)	exp
1 $^1B_{3u}$	Q_x	3.61	1.14	1.98−2.02	3.56	1.61	1.81
1 $^1B_{2u}$	Q_y	3.87	1.89	2.33−2.42	3.49	1.99	1.99
2 $^1B_{3u}$	B_x	5.20	2.51	3.31−3.33	5.63	3.14	3.65
2 ^{1}B2u	B_y	5.23	3.21		6.14	3.19	

(for the leveling of the components, the two central H atoms define the *X* axis and the *Z* axis is defined to be perpendicular to the molecular plane). Although, bands called N and L have been observed over B, the current study is limited to the first excited states because the aim is to compare two molecules, one of them of large size. The first outcome that can be summarized is that the CAS method produces too high values for the positions whereas the CASPT2 produces too low values. As the correlation and the active space increase, the full spectrum is displaced to the low energies.

The Q_x and Q_y bands have been always assigned to the transitions to the 1 B_{3u} and 1 B_{2u} electronic states.[39−45] However, two different assignments have been suggested for the B band. In the traditional interpretation, based on the four orbital model, the B band is contemplated as a superposition of two B_x and B_y unsolved components who are assigned to the transitions to the $2B_{3u}$ and $2B_{2u}$ states.[11,19,38−40] The second interpretation proposes the calculations produce a gap between the B_x and B_y components that is not observed experimentally. B is interpreted as a single component that can be assigned to the $2B_{3u}$ state and the transition to 2 B_{2u} state is assigned to the N band.[16] The main group of authors accept the traditional theory and the splitting between B_x and B_y is explained[19] as a basis set error that can be eliminated by improving the level of calculations. By comparing our 6-31G(d,p) (5D) and 6-31G results, we can infer the same outcome (see Tables 5 and 6).

Some undesirable results that block a definitive interpretation of the PH_2 spectrum are found. The splitting between the calculated B_x and B_y components increases with the improvement of the space. It has been calculated to be 0.01 eV with the CAS(4,4) model and to be 0.46 eV with CAS(15/26) one. In addition, the dynamical correlation augments the splitting from 0.01 to 1.09 eV for the CAS(4/4) space, although the effect disappears using the 5 orbital model. In this case, it has been found to be 0.09 and 0.1 eV with CAS and CASPT2 and the N band has been calculated at 4.12 eV, really separated fom B. This result agrees with the one obtained with the 13 and 14 orbital models of ref 19. Whereas current data support the traditional interpretation, a definitive assignment cannot be done for the moment and requires new high-resolution experimental data and calculations of the exited states with full optimization of the geometry, which is implausible given the size of the molecules.

In Table 6, the spectra of PH_2 and PcH_2 are determined with the four orbital model (see Figure 4) and the 6-31G basis set. The model is extended for PcH_2 although it has been disregarded[28] given the high density of states around HOMO−1 that are neglected.[28] This is the case of the π orbitals HOMO−2, ..., HOMO−8, lying between 9 and 10 eV. However, although it is evident that the four orbital space is too limited for a multiconfigurational calculation, it has to be considered that all the valence orbitals are correlated with the CASPT2 method. The latest dynamical correlation introduced by perturbation theory corrects the error and justifies the extremely good agreement between the CASPT2 results and the experimental ones.

Concerning the density of states, the electronic configurations of both molecules present clear differences. The LUMO−HOMO gap is 0.67 eV for PcH_2 and 6.54 eV for PH_2. The gap HUMO−HUMO−1 is 0.21 eV for PH_2 and 3.31 eV for PcH_2. For PcH_2, almost a single configuration contributes to the excited states, whereas, in PH_2, two configurations contribute. Two transitions contribute with a weight of ≈50% to the bands of PH_2, whereas a unique transition contribute with a weight of ≈90% to the bands of PcH_2:

	PH_2	PcH_2		PH_2	PcH_2
Q_x	$2a_u \rightarrow 4b_{3g}$ $5b_{1u} \rightarrow 4b_{2g}$	$4a_u \rightarrow 6b_{3g}$	Q_y	$2a_u \rightarrow 4b_{2g}$ $5b_{1u} \rightarrow 4b_{3g}$	$4a_u \rightarrow 6b_{2g}$
B_x	$2a_u \rightarrow 4b_{3g}$ $5b_{1u} \rightarrow 4b_{2g}$	$6b_{1u} \rightarrow 6b_{2g}$	B_y	$2a_u \rightarrow 4b_{2g}$ $5b_{1u} \rightarrow 4b_{3g}$	$6b_{1u} \rightarrow 6b_{3g}$

The CASPT2 results are in very good agreement with the experimental values and allow us to interpret the spectrum of PcH_2. The positions of the three bands, Q_x, Q_y, and B, observed at 1.81, 1.99, and 3.65 eV,[32] have been calculated at 1.61, 1.99, and 3.14−3.19 eV. It may be predicted that an extension of the active space up to HOMO−8 can stabilize the $2B_{3u}$ and $2B_{2u}$ states and approach the B band to the experimental value.

Acknowledgment. We acknowledge the CSIC of Spain and the CITMA of Cuba for the grant 2001CU0010. This work has been also supported bi the Ministerio de Ciencia y Tecnología of Spain, grants AYA2002-02117 and BFM2001-2315.

Supporting Information Available: Table of harmonic frequencies of PH_2 and PcH_2 calulated with B3LYP/6-31G(d,p) (5D). This material is available free of charge via the Internet at http://pubs.acs.org.

References and Notes

(1) Dolphin, D., Ed. *The Porphyrins*; Academic Press: New York, 1978/1979; Vols. 1−7.

(2) Leznoff, C. C., Lever, A. B. P., Eds. *Phthalocyanines. Properties and Applications*; VCH: Weinheim, 1989−1993; Vols. 1−3.

(3) Amstrong, N. R. *J. Porphyrins Phthalocynines* **2000**, *4*, 414

(4) Nagashima, U.; Takada, T.; Ohno, K. *J. Chem. Phys.* **1986**, *85*, 4524

(5) Reynolds, C. H. *J. Org. Chem*. **1988**, *53*, 6061.

(6) Li, X.; Zgierski, M Z. *J. Phys. Chem.* **1991**, *95*, 4268.

(7) Foresman, J. B.; Head-Gordon, M.; Pople J. A.; Frisch, M. J. *J. Phys. Chem.* **1992**, *96*, 135.

(8) Yamamoto, Y.; Noro T.; Ohno K. *Int. J. Quantum Chem*. **1992**, *42*, 1563.

(9) Almlof, J.; Fisher, T. H.; Gassnman, P. G.; Ghost A.; Häser, M. *J. Phys. Chem*. **1993**, *97*, 10964.

(10) Merchán M.; Ortí E.; Roos B. O. *Chem. Phys. Lett*. **1994**, *221*, 136.

(11) Merchán M.; Ortí E.; Roos B. O. *Chem. Phys. Lett*. **1994**, *226*, 27.

(12) Ghosh, A.; Almlöf, J. *J. Phys. Chem*. **1995**, *99*, 1073.

(13) Radziszewski, J. G.; Nepras, M.; Balaji, V.; Waluk, J.; Vogel E.; Michl, J. *J. Chem. Phys*. **1995**, *99*, 14254.

(14) Mozlowski, P. M.; Zgierski, M. Z.; Pulay P. *Chem. Phys. Lett.* **1995**, *247*, 379.

(15) Kozlowsky, P. M.; Jarzcki A. A.; Pulay, P. *J. Phys. Chem*. **1996**, *100*, 7007.

(16) Nakatsuji, H.; Hasegawa, J.; Hada, H. *J. Chem. Phys*. **1996**, *104*, 2321.

(17) Nooijen, M.; Bartlett, R. J. *J. Phys. Chem*. **1997**, *106*, 6449.

(18) Ghosh, A. *Acc. Chem. Res*. **1998**, *31*, 189.

(19) Serrano-Andrés, L.; Merchán, M.; Rubio, M.; Roos, B. O. *Chem. Phys. Lett.* **1998**, *295*, 195.

(20) Gwaltney R.; Bartlett, R. J. *J. Chem. Phys.* **1998**, *108*, 6790.

(21) Tokita, Y.; Hasegawa, J.; Nakatsuji, H. *J. Phys. Chem. A* **1998**, *102*, 1843.

(22) van Gisgergen, S. J. A.; Rosa, A.; Ricciardi, G.; Baerends, E. J. *J. Chem. Phys.* **1999**, *111*, 2499.

(23) Tazi, M.; Lagant, P.; Vergoten, G. *J. Phys. Chem. A* **2000**, *104*, 618.

(24) Parusel, A. B. J.; Ghosh, A. *J. Phys. Chem. A* **2000**, *104*, 2504.

(25) Maity, D. K.; Truong, T. N. *J. Porphyrins Phthalocyanines* **2001**, *5*, 289.

(26) Lee, L. K.; Sabelli, N. H.; LeBreton, P. R. *J. Phys. Chem*. **1982**, *86*, 3926.

(27) Ortí, E.; Brédas, J. L. *J. Chem. Phys.* **1988**, *89*, 1009.

(28) Ortí, E.; Brédas, J. L. *J. Chem. Phys.* **1990**, *92*, 1228.

(29) Robertson, J. M. *J. Chem. Soc.* **1936**, 1195.

(30) Hoskins, B. F.; Mason, S. A.; White, J. C. B. *J. Chem. Soc., Chem. Commun*. **1969**, 554.

(31) Fleischer, F. B. *Acc. Chem. Res*. **1970**, *3*, 105.

(32) Edwards, L.; Gouterman, M. *J. Mol. Spectrosc.* **1970**, *33*, 292.

(33) Martin, K. A.; Stillman, M. J. *Can. J. Phys.* **1979**, *57*, 1111.

(34) Berkowitz, J. *J. Chem. Phys*. **1979**, *70*, 2819.

(35) Chen, B. M. L.; Tulinsky, A. *J. Am. Chem. Soc.* **1972**, *94*, 4144.

(36) Crossley, M. J.; Harding, M. M.; Sternhell, S. *J. Am. Chem. Soc*. **1992**, *114*, 3266.

(37) Cicek, J.; Paldus, J. *J. Chem. Phys.* **1967**, *47*, 3976.

(38) Gouterman, M. *J. Chem. Phys*. **1959**, *30*, 1139.

(39) Gouterman, M.; Wagnière, G.; Synder, L. C. *J. Mol. Spectrosc*. **1963**, *11*, 108.

(40) Weiss, C.; Kobayashy, H.; Gouterman, M. *J. Mol. Spectrosc*. **1965**, *16*, 415.

(41) Rimington, C.; Mason, S. F.; Kennard, O. *Spectrochim. Acta* **1958**, *12*, 65.

(42) Anex, B. G.; Umans, R. S. *J. Am. Chem. Soc.* **1964**, *86*, 5026.

(43) Edwards, L. E.; Dolphin, D. H.; Gouterman, M. *J. Mol. Spectrosc*. **1970**, *35*, 90.

(44) Edwards, L.; Dolphin, D. H.; Gouterman, M.; Adler, A. D. *J. Mol. Spectrosc.* **1971**, *38*, 16.

(45) Kim, B. F.; Bohandy, J. *J. Mol. Spectrosc*. **1978**, *73*, 332.

(46) Frisch, M. J.; Trucks, G. W.; Schlegel, H. B.; Scuseria, G. E.; Robb, M. A.; Cheeseman, J. R.; Zakrzewski, V. G.; Montgomery, Jr. J. A.; Stratmann, R. E.; Burant, J. C.; Dapprich, S.; Millam, J. M.; Daniels, A. D.; Kudin, K. N.; Strain, M. C.; Farkas, O.; Tomasi, J.; Barone, V.; Cossi, M.; Cammi, R.; Mennucci, B.; Pomelli, C.; Adamo, C.; Clifford, S.; Ochterski, J, Petersson, G. A.; Ayala, P. Y.; Cui, Q.; Morokuma, K.; Salvador, P.; Dannenberg, J. J.; Malick, D. K.; Rabuck, A. D.; Raghavachari, K.; Foresman, J. B.; Cioslowski, J.; Ortiz, J. V.; Baboul, A. G.; Stefanov, B. B.; Liu G.; Liashenko, A.; Piskorz, P.; Komaromi, I.; Gomperts, R.; Martin, R. L.; Fox, D. J.; Keith, T.; Al-Laham, M. A.; Peng, C. Y.; Nanayakkara, A.; Challacombe, M.; Gill, P. M. W.; Johnson, B.; Chen, W.; Wong, M. W.; Andres, J. L.; Gonzalez, C.; Head-Gordon, M.; Replogle, E. S.; Pople, J. A. *Gaussian 98*, revision A.1x; Gaussian, Inc.: Pittsburgh, PA, 2001.

(47) Seeger, R.; Pople, J. A. *J. Chem. Phys.* **1977**, *66*, 3045.

(48) Nakatsuji, H.; Hirao, K. J. *J. Chem. Phys.* **1978**, *68*, 2035.

(49) Ghosh, A.; Gassman, P. G.; Almlöf, J. *J. Am. Chem. Soc.* **1994**, *116*, 1932.

(50) Piet, D. P.; Danovich, D.; Zuilhof, H.; Sudhölter, E. J. R. *J. Chem. Soc., Perkin Trans.* **1999**, *2*, 1653.

(51) MOLCAS Version 5. K. Andersson, M. Barysz, A. Bernhardsson, M. R.A. Blomberg, D. L. Cooper, T. Fleig, M. P. Fülscher, C. de Graaf, B. A. Hess, G. Karlström, R. Lindh, P.-Å. Malmqvist, P. Neogrády, J. Olsen, B. O. Roos, A. J.Sadlej, M.Schütz, B. Schimmelpfennig, L. Seijo, L. Serrano-Andrés, P. E. M. Siegbahn, J. Stålring, T. Thorsteinsson, V. Veryazov, P.-O. Widmark, Lund University, Sweden, 2000.